JOURNAL OF THE AMERICAN WATER RESOURCES ASSOCIATION
Vol. 44, No. 4 AMERICAN WATER RESOURCES ASSOCIATION August 2008

STOCHASTIC TRANSFER FUNCTION MODEL AND NEURAL NETWORKS TO ESTIMATE SOIL MOISTURE[1]

Nazario D. Ramírez-Beltran, Joan Manuel Castro, Eric Harmsen, and Ramón Vásquez[2]

ABSTRACT: A practical methodology is proposed to estimate the three-dimensional variability of soil moisture based on a stochastic transfer function model, which is an approximation of the Richard's equation. Satellite, radar and *in situ* observations are the major sources of information to develop a model that represents the dynamic water content in the soil. The soil-moisture observations were collected from 17 stations located in Puerto Rico (PR), and a sequential quadratic programming algorithm was used to estimate the parameters of the transfer function (TF) at each station. Soil texture information, terrain elevation, vegetation index, surface temperature, and accumulated rainfall for every grid cell were input into a self-organized artificial neural network to identify similarities on terrain spatial variability and to determine the TF that best resembles the properties of a particular grid point. Soil moisture observed at 20 cm depth, soil texture, and cumulative rainfall were also used to train a feedforward artificial neural network to estimate soil moisture at 5, 10, 50, and 100 cm depth. A validation procedure was implemented to measure the horizontal and vertical estimation accuracy of soil moisture. Validation results from spatial and temporal variation of volumetric water content (vwc) showed that the proposed algorithm estimated soil moisture with a root mean squared error (RMSE) of 2.31% vwc, and the vertical profile shows a RMSE of 2.50% vwc. The algorithm estimates soil moisture in an hourly basis at 1 km spatial resolution, and up to 1 m depth, and was successfully applied under PR climate conditions.

KEY TERMS: soil moisture; transfer function; neural networks; sequential quadratic programming; vertical profile.

Ramírez-Beltran, Nazario D., Joan Manuel Castro, Eric Harmsen, and Ramón Vásquez, 2008. Stochastic Transfer Function Model and Neural Networks to Estimate Soil Moisture. *Journal of the American Water Resources Association* (JAWRA) 44(4):847-865. DOI: 10.1111/j.1752-1688.2008.00208.x

INTRODUCTION

Soil moisture is a fundamental component of the surface water and energy budget. The soil moisture regulates the partition of latent and sensible heat fluxes at the surface, affecting the boundary layer. Usually, atmospheric models do not consider the state and evolution of the soil moisture. Thus, using incorrect soil-moisture initial conditions may generate misleading modeling results. For instance Balsamo *et al.* (2004) reported that erroneous estimation of total soil moisture affected the quality of the forecast for several days when using a numerical weather prediction scheme. It is also well known that soil moisture plays an important role in detection and attribution of

[1]Paper No. J06139 of the *Journal of the American Water Resources Association* (JAWRA). Received October 13, 2006; accepted February 7, 2008. **Discussions are open until February 1, 2009**.

[2]Respectively, Professor, Department of Industrial Engineering, University of Puerto Rico, Mayaguez, PR 00680; (Castro and Vásquez) Graduate Student and Dean, Department of Electrical and Computer Engineering, University of Puerto Rico, Mayaguez, PR 00680; (Harmsen) Professor, Department of Agricultural and Biosystems Engineering, UPRM, PR 00680 (E-mail/Ramírez-Beltran: nazario@ece.uprm.edu).

global climate changes (Huang *et al.*, 1996). Recently, several agencies and universities have been organized to conduct land data assimilation system (LDAS) that intends to enhance soil and temperature initial conditions for numerical weather/climate prediction models by using real-time observed precipitation and solar insolation data (Fan *et al.*, 2002; Robock *et al.*, 2003; Margulis *et al.* 2002; Walker and Houser, 2004; Belair *et al.*, 2005; McKee *et al.*, 2001). Soil moisture is not only an important variable for modeling but also has important practical applications, including water resource management, reservoir design and operation, drought assessment, flood forecasting, crop production, irrigation, and forest yield estimation (Dinar *et al.*, 1986; Mehrotra, 1999; Viterbo and Betts, 1999).

There are several physically based soil-moisture models and most of them are based on the Richard's equation. The Richard's equation represents the dynamic distribution of pore water pressure in partially saturated soils (Yeh *et al.*, 1998; Lee and Abriola, 1999; Kumar, 2004). The water balance approach attempts to estimate the soil-moisture content in a simplified way, thus, greatly reducing the computational effort (Huang *et al.*, 1996; Van den Dool *et al.*, 2003; MIKE SHE, DHI Software, Inc., 2003; Ross *et al.*, 2004; Downer *et al.*, 2003).

Since some variables/parameters of the Richard's equation are not accurately known, stochastic models may help to represent uncertainties. Thus, a stochastic representation of the Richard's equation was introduced by Entekhabi and Rodriguez-Iturbe (1994) and later modified by Castelli *et al.* (1996) and Pan *et al.* (2003). Our proposed model is an approximation of the stochastic version of the Richard's equation.

Entekhabi and Rodriguez-Iturbe (1994) have shown that the rainfall is the principal driver that controls the state and evolution of the soil moisture, and based on this observation, Pan *et al.* (2003) proposed a method for estimating soil moisture. They represented the soil-moisture dynamics by a linear stochastic partial differential equation. They also eliminated the diffusion term to simplify the stochastic equation and express the soil moisture as a function of the time-weighted average of the previous cumulative rainfall over a given period.

Although precipitation is the primary force controlling the state and evolution of the soil moisture, its estimation requires studying the soil and vegetation properties. For instance, Pan's method requires estimation of three parameters: the window size, the infiltration parameter, and the loss parameter. The window size was determined by observing the linear relationship between the soil moisture and the average of the previous cumulative rainfall. The infiltration parameter was estimated by using an empirical relationship between the observed mean soil moisture and the mean of the previous cumulative rainfall. The loss parameter was determined using an empirical function of the saturated hydraulic conductivity and the leaf area index. It is obvious that to represent the spatial and temporal variability of the soil moisture requires including properties of the soil and vegetation. Therefore, our model includes the following variables: rainfall, soil texture, surface temperature, vegetation index, and topography.

Walker *et al.* (2002) introduced a modified Kalman Filter to retrieve the soil moisture profile in a 6 ha catchment performing measurements at five different depths from the surface to 1 m depth. They determined that the soil-moisture profile cannot be retrieved from near-surface soil-moisture measurements when the near surface and deep soil layers become decoupled, such as during extreme drying events. We are also exploring the possibility of estimating the soil-moisture profile for PR based on near-surface soil-moisture measurements.

We are using a self-organized neural network (SONN) to identify spatial similarities among grids and a feedforward artificial neural network (ANN) to estimate the soil moisture at different depths. An ANN is selected to estimate soil-moisture profile because the dynamic water content of soil is a nonlinear process and the ANN has been proven to be an efficient estimation approach when the variables of a system are related in a highly nonlinearly way (Zongqian *et al.*, 2000; Satalino *et al.*, 2002; Gill *et al.*, 2006). The ANN technique is a general nonlinear modeling approach that is based on nonlinear optimization algorithms (Hagan *et al.*, 1996). An ANN determines an empirical relationship between the inputs and outputs of a given system. Therefore, it is important that the user has a good understanding of the science behind the underlying system to provide the appropriate inputs, and consequently to support the identified relationship. It should be mentioned that the physically based models provide the theoretically representation of the soil-moisture dynamics. The ANN may help to develop reasonable estimates when sufficient and appropriate information is provided. Thus, the key issue to obtain a successful ANN application is to select the appropriate training variables and to identify a suitable ANN structure. The structure of the ANN consists of determining the number of layers, the number of neurons in the hidden layers, and selecting the best activation function for each layer. We implemented an efficient procedure to identify the appropriate structure of a neural network (Ramirez-Beltran and Montes, 2002).

An interesting application of the ANN to estimate soil moisture is presented by Satalino *et al.* (2002). They studied the feasibility of retrieving soil-moisture

content over smooth bare-soil fields using European Remote Sensing synthetic aperture radar (ERS-SAR) data. The retrieval approach consists of inverting the integral equation method by using an ANN. The overall root mean square error in the retrieved volumetric soil-moisture content was ±6%. They have reported that the major source of soil-moisture estimation is the roughness conditions, which influences the relationship between soil-moisture coefficient and the radar backscattering coefficient. Jiang and Cotton (2004) implemented an ANN technique for soil-moisture estimation. They used daily precipitation, vegetation index, cloud-mask infrared skin temperature, and soil-moisture profile. They found a high correlation between ANN estimates and the actual observations, and they claim that the ANN-based technique is capable of estimating soil moisture from remotely sensed impulse response (IR) data with high spatial and temporal resolution.

This paper is organized as follows: the second section shows Puerto Rico climate conditions and describes the *in situ* and remote sensing data used to build the soil-moisture model. The third section describes the stochastic TF and the parameter estimation procedure, illustrates the use of a SONN to identify similarities among grids to select the appropriate TF, and shows the use of a feedforward ANN to estimate soil moisture at different depths. The fourth section presents the results of the PR soil-moisture analysis. The fifth section describes some potential applications of the soil moisture, and the last section presents a summary and some conclusions.

PUERTO RICO CLIMATE CONDITIONS AND DATA

The proposed methodology was implemented for the climatological conditions of PR. PR is part of the Greater Antilles island chain and is located in the northeastern Caribbean Sea. Precipitation is primarily affected by troughs imbedded in easterly waves during summer months and cold fronts during winter months. Life zone studies show that PR is characterized by having subtropical dry forest (17%), subtropical moist forest (58.4%), subtropical wet forest (22.6%), subtropical rain forest (0.1%), lower mountain wet forest (1.2%), and lower mountain rain forest (0.1%), (Ewel and Whitmore, 1973). Although PR is a small island, 30 vegetation classes and approximately 400 soil series have been identified (Helmer, 2002). PR includes 8,700 km^2 in which the spatial and temporal variability of soil moisture is primarily associated with complex vegetation, soil texture, surface temperature, topography, and precipitation.

Essentially two major data sources were used as part of the soil-moisture study: a local soil-moisture measurement network and rainfall rates obtained from the Next Generation Weather Radar (NEXRAD).

Soil-Moisture Network

The locations of the soil-moisture stations used in this study are shown in Figure 1. The soil-moisture network included 17 stations, 12 of which were owned and operated by the University of PR-Mayagüez (UPRM) research project and the remaining five were owned and operated by the Natural Resources Conservation Services (NRCS). The latter five stations are part of the Soil Climate Analysis Network (SCAN) that covers United States (U.S.) and PR. The UPRM stations collected hourly observations during the period from 2005 to present and includes soil moisture, air temperature, and rainfall. These stations include three ECHO-20 soil-moisture sensors that collect information at 20 cm depths, an ECHO temperature sensor located at 20 cm height, an ECRN-50 rain gauge, and a data logger that collects the information from the five sensors every hour. Detailed description of the used sensors can be found at: http://www.decagon.com/Ech2o. The NRCS stations also collect the following parameters on an hourly basis: soil moisture and soil temperature at 5, 10, 20, 50, and 100 cm depth, air temperature, rainfall, solar radiation, wind speed, and wind direction (http://www.wcc.nrcs.usda.gov/scan/). Most of the PR-SCAN stations have been installed during the period 2004-2006; however, there are some of them that have collecting soil-moisture information since 1994. An experimental field campaign was conducted to collect undisturbed soil samples in the neighborhood

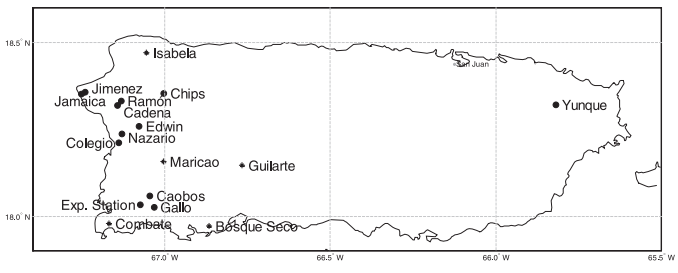

FIGURE 1. Location of Soil-Moisture Stations in PR. Stars and dots represent the location of the NRCS and project station (UPRM), respectively.

of stations to measure volumetric water content and calibrate the soil-moisture sensors.

NEXRAD Rainfall Data

One of the NEXRAD network components of the National Weather Service of the U.S. is located in PR. NEXRAD Stage III grids are stored in a binary file format called xmrg. Rainfall data were obtained by using the multisensor precipitation estimation (MPE) algorithm, which was developed by the Hydrologic Research Laboratory (Breidenbach and Bradberry, 2001). The xmrg is a MPE product that uses radar precipitation and rain gauge measurements to derive the best estimators of rainfall for specific area and time. The xmrg product provides hourly rainfall.

It is well known that there are some difficulties associated with radar rainfall estimation (Hunter, 1996; Fulton *et al.*, 1998; Westrick *et al.*, 1999). High and low radar reflectivity caused by mountainous region lead to underestimation or overestimation of rainfall (Klazura *et al.*, 1999). Also the low spatial resolution, the detection from the antenna, and the elevation angle of the radar beams reduces accuracy. The authors are currently conducting a validation of the NEXRAD rainfall over PR.

In addition to the soil-moisture network, PR has a rain gauge network that includes 125 sensors across the island that provides rainfall records every 15 min. NEXRAD level III data provide rainfall estimates every 6 min with 1 km spatial resolution. Rainfall comparison was performed between a rain gauge and the nearest grid to the corresponding rain gauge. Preliminary validation has been conducted over seven heavy storms. The hit rate indicates that 90% of the time the NEXRAD indicates correctly when rainfall events are present or absent. However, the probability of detection (POD) showed that 42% of the time the NEXRAD detects the presence of rainfall events. Thus, the selected storms covered only part of the island, and the validation process was dominated by the absence of rain in many rain gauges, that coincided with the absence of reflectivity in the corresponding grids and consequently the hit rate was large with low POD. The false alarm rate showed that 35% of the time the NEXRAD indicated rainfall events when in reality there was no rain. The measurement accuracy in terms of the amount of rainfall reveals that the RMSE was 1.64 mm for the 15 min estimates. The bias ratio of the NEXRAD was 0.75, which indicates that on average the NEXRAD incurred an underestimation of 25%. It should be pointed out that the NEXRAD rainfall errors will increase the soil-moisture estimation errors in our proposed methodology. In the near future, this error will be studied to determine how the rainfall errors propagate over the soil-moisture estimates.

METHODOLOGY

The Soil-Moisture Model

One of the purposes of this work is to develop a soil-moisture estimation model for tropical areas such as PR, which has complex topography, tropical vegetation, and persistent cloud cover. The formulation of the model is based on the observation that precipitation is the paramount force controlling the state and evolution of soil moisture.

Entekhabi and Rodriguez-Iturbe (1994) have shown that the soil-moisture vertical profile can be derived by using the stochastic version of the well known Richard's equation (Lee and Abriola, 1999; Kumar, 2004), which can be represented by a linear stochastic partial differential equation. Pan *et al.* (2003) proposed a similar linear stochastic partial differential equation to model the soil-moisture dynamics. They have shown that the intrinsic dynamics of volumetric soil-moisture $h(x, t)$ is driven by the rainfall rate $p(x, t)$ and is given by

$$Z\frac{\partial h}{\partial t} = -\eta h + Z(\kappa\nabla^2 h) + \gamma P_{\text{net}}(x,t), \tag{1}$$

where Z is the thickness of the soil layer, t is the time, η is the loss coefficient, κ is the diffusion coefficient, $\kappa\nabla^2 h$ is the diffusion term, γ is the infiltration coefficient, and $P_{\text{net}}(x, t)$ is the net rainfall rate.

It should be noted that the net rainfall rate is equal to the differences between the rainfall rate and the interception, i.e., for a nonforested region $P_{\text{net}}(x, t) \approx p(x, t)$. Entekhabi and Rodriguez-Iturbe (1994) have shown that diffusion is small compared to vertical losses because of the evapotranspiration and percolation. In addition, Pan *et al.* (2003) have come to the conclusion that if the soil moisture is to be computed for times scale of one day or less, the diffusion term can be neglected. Thus, they dropped the diffusion term and estimated the net rainfall rate by the cumulative rain that occurs in a short time interval (i.e., $P_{\text{net}}(x,t) = \frac{\Delta P(x)}{\Delta t}$). They also have assumed that η and γ are independent of time and $\frac{\Delta P(x)}{\Delta t}$ is constant during the time period from t to $t + \Delta t$, where Δt is a short time interval. Thus, Pan *et al.* (2003) finally show that equation (1) is reduced to the following stochastic ordinary differential equation.

$$Z\frac{\mathrm{d}h}{\mathrm{d}t} = -\eta h + \gamma\frac{\Delta P}{\Delta t} \tag{2}$$

Thus, equation (2) for a given location x can be written as follows:

$$\frac{\mathrm{d}h(t)}{\mathrm{d}t} = -k_1 h(t) + k_2 R_L(t), \quad k_1 > 0, \tag{3}$$

where $k_1 = \frac{\eta}{Z}$, $k_2 = \frac{\gamma}{Z}$ and $R_L(t) = \frac{\Delta P}{\Delta t}$.

In the previous equations $h_t(t)$ and $R_L(t)$ were considered as continuous functions, but in practice, there are usually discrete data h_t and $R_{L,t}$. It has been shown that a first-order differential equation could be written as a first-order difference equation (Box and Jenkins, 1976; Pandit and Wu, 1983; Wei, 1990; Hamilton, 1994; Spiegel, 1994; Brockwell and Davis, 2002). Thus, equation (3) can be approximated as follows:

$$h_t = -\phi h_{t-1} + \theta R_{L,t}, \quad \phi > 0, \tag{4}$$

where h_t is the soil moisture at time t and $R_{L,t}$ is the accumulated rainfall at time t during the last L times periods, ϕ and θ are constant coefficients.

Although Equation (4) provides an approximation of the soil-moisture dynamics, it was noted that the stochastic TF model provides a better representation of the soil-moisture behavior. The stochastic TF model is a difference equation and the relationship between the continuous and discrete TFs were also discussed by Pandit and Wu (1983) and Box and Jenkins (1976). The discrete stochastic TF model equivalent to Equation (4) is given as follows:

$$h_t = \upsilon_1(B)h_{t-1} + \upsilon_2(B)r_t + \varepsilon_t, \tag{5}$$

where

$$\upsilon_j(B) = \frac{\omega_j(B)}{\delta_j(B)} = \frac{\omega_{j,0} + \omega_{j,1}B + \omega_{j,2}B^2 + \cdots + \omega_{j,S}B^S}{1 - \delta_{j,1}B - \delta_{j,2}B^2 - \cdots - \delta_{j,r}B^r}, \quad j = 1, 2 \tag{6}$$

where $\upsilon_1(B)$ and $\upsilon_2(B)$ are the IR functions, and B is the back shift operator, $B^d x_t = x_{t-\mathrm{d}}$, and d is an integer value. The variable r_t is the accumulated rainfall during 15 min., and it will be called instantaneous rainfall at time t, and ε_t is a sequence of independent random variable with mean zero and constant variance, this random error takes into account uncertainties for unobservable variables that are not included in the soil-moisture model. It should be noted that r_t is used instead of $R_{L,t}$ as the accumulation of rainfall is carried out by the IR function $\upsilon_2(B)$. The first IR function is a set of coefficients associated with the previous soil-moisture dynamics, the loss coefficient, and a particular thickness of the soil layer; whereas, the second IR function is related to cumulative and instantaneous rainfall values, infiltration coefficient, and a given thickness of the soil layer.

Experimental results were used to modify the second IR function. We observed that the level of the soil moisture is primarily controlled by the antecedent soil-moisture values and the sudden soil-moisture response is modeled by cumulative and instantaneous rainfall effects, simultaneously. It is noted that if the precipitation during consecutive days is not present and the soil is relatively dry (i.e., close to wilting point) a significant rainfall event will produce a relatively large increase in the soil moisture. On the other hand, if several rainfall events occurred frequently during the previous few days then the soil-moisture response is relatively small because of the soil moisture already being near the field capacity or possibly the saturation point. Therefore, the second IR function can be written in the following form:

$$\upsilon_2(B) = \frac{\omega_2(B)}{\delta_2(B)}\mathrm{e}^{-\tau \mathrm{R}_{\mathrm{L},t}}, \tag{7}$$

where the integer variable L is obtained during the parameter estimation process, and τ is the attenuation parameter that modulates the soil-moisture response associated with an instantaneous rainfall event. Thus, if no rainfall events occur during the previous days, the $R_{L,t}$ will be zero and the soil-moisture response will be large because of instantaneous rainfall. On the other hand, if frequent rainfall events occurred during the previous days, then the $R_{L,t}$ will be greater than zero and the soil-moisture response will be attenuated by the exponential term. Consequently, a stochastic TF model that expresses the soil-moisture dynamics for a particular layer and location can be written as follows:

$$h_t = \left(\frac{\omega_{0,1} + \omega_{0,2}B}{1 - \delta_{0,1}B - \delta_{0,2}B^2}\right)h_{t-1} + \left(\frac{\omega_{1,1} + \omega_{1,2}B}{1 - \delta_{1,1}B}\right)r_t\mathrm{e}^{-\tau R_{L,t}} + \varepsilon_t, \quad \tau > 0, \tag{8}$$

where the involved variables and parameters were defined in Equations (4, 5, and 7).

Equation (8) can be used to estimate the soil moisture when a large number of soil-moisture stations are available (i.e., the extreme soil-moisture values are involved in the parameter estimation process). However, in practices, to accomplish this task is difficult,

and consequently, the upper and lower values of the TF model should be limited by the saturated and wilting points, respectively. Therefore, for a given grid point, the following stochastic TF model is proposed:

$$h_t = \rho + (\psi - \rho)(1 - e^{-f_t}), \tag{9}$$

where

$$f_t = \left(\frac{\omega_{0,1} - \omega_{0,2}B}{1 - \delta_{0,1}B}\right) f_{t-1} + \left(\frac{\omega_{1,1} - \omega_{1,2}B}{1 - \delta_{1,1}B}\right) r_t e^{-\tau R_{L,t,}} \quad f_t > 0 \tag{10}$$

$$\rho = 18.74 + 0.00315(si\,c) - 0.146\,s \tag{11}$$

$$\psi = 33.2 - 7.251 \times 10^{-2} s + 12.76 \log_{10}(c), \tag{12}$$

where ρ and ψ are approximations of the permanent wilting point, and the saturation point at a given location, respectively; c, s, and si are the percentage of clay, sand, and silt at a particular grid. The geopedestrain equations were tested for PR soil and climatic conditions and successful results were found. The equation of wilting point was proposed by Cemek *et al.* (2004) and the saturation point by Strait *et al.* (1979).

It should be pointed out that to derive estimates for Equation (10) it may be used the relationship between the observed soil moisture with the f_t function as follows:

$$f_t = -\ln\left(\frac{\psi - h_t}{\psi - \rho}\right) \tag{13}$$

Analysis of the IR Function

The IR function is defined by the division of two polynomials ω_j(B) and $\delta_j(B)$ (see Equation 6), and this division creates an infinite time series that converges when the system is asymptotical stable (Pandit and Wu, 1983). The rational representation of the TF is a parsimonious model and the evaluation of the TF is given by a long division of two polynomials, in which only the most significant values are considered. The asymptotic stability of the TF is measured by computing the roots of the polynomial on B ($\delta_j(B) = 0$). It has been shown that the system is asymptotically stable if the roots of ($\delta_j(B) = 0$) fall outside of the unitary circle (Pandit and Wu, 1983).

The persistence of the soil moisture in a given area will be called the memory of the soil moisture. Thus, if the water last for a long period of time in the soil, it will be referred as long soil-moisture memory; on the contrary, it will be referred as the short soil-moisture memory. The memory of the soil moisture is controlled by the sum of two products: $\upsilon_1(B)f_{t-1}$ and $\upsilon_2(B)r_t$. To analyze the influence of the IR function on the memory of the soil moisture considered a single function that can take the form of either $\upsilon_1(B)$ or $\upsilon_2(B)$ and for simplicity will be called $\upsilon(B)$:

$$\upsilon(B) = \frac{\omega_0 + \omega_1 B}{1 - \delta B} \tag{14}$$

The contribution of the IR function to memory of the soil moisture is essentially controlled by the δ-value. This is the result of the fact that

$$\upsilon(B) = \frac{\omega_0 + \omega_1 B}{1 - \delta B} = (\omega_0 + \omega_1 B)(1 + \delta B + \delta^2 B^2 + \cdots) = \lambda_1 + \lambda_2 B + \lambda_2 B^2 + \cdots = \sum_{i=1}^{\infty} \lambda_i B^{i-1} \tag{15}$$

It should be noted that when delta is negative, the geometric series alternates the sign and reduces the response in the soil moisture (i.e., reduces the memory of the soil moisture).

Assuming that the omega parameters are both positives and delta approaches to positive one, the soil-moisture persistence effect will last for long time period (i.e., long memory). In addition, if omega parameters are both negatives and delta approaches to negative one, the soil moisture will have long memory. On the other hand, if delta approaches to zero, then the persistence effect will last a very short period of time (short memory).

Parameter Estimation

A TF model was identified for each station, assuming that the parameters of the IR function characterize the terrain properties for a given location. Thus, it is assumed that $\omega's$, $\delta's$, τ, and L are parameters that exhibit inherent terrain characteristics of a specific location, and consequently, the spatial variability is expressed by the parameters of the IR functions. Thus, evaluating the TF model in another location that exhibits similar terrain characteristics (as determined by the self-organized neural network) will estimate the response of the soil-moisture dynamics.

There is a well known and systematic procedure to perform parameter estimation of the TF model when it has only one input variable. In this case, there are two input variables in addition to an exponential term and consequently, conventional techniques (Box and Jenkins, 1976; Pandit and Wu, 1983; Wei, 1990) to perform parameter estimation cannot be applied. The estimation of the transfer-function parameters is not a trivial task, it requires a well-planned procedure. We are proposing a general procedure to estimate parameters for a multivariate TF model with nonlinear terms. The estimation procedure includes five main steps:

1. The first step consists of applying the periodgram and the autocorrelation function to determine whether or not the transformed soil moisture, f_t, is a stationary process. Typically, the soil moisture is a nonstationary process because of significant changes of the mean that have occurred over the time, because of rainfall long-term impact over the soil-moisture response. The process becomes stationary after the trend is removed. This is accomplished by taking the first, $(1-B)f_t$, or the second, $(1-B)^2 f_t$, difference to the process or by removing a parametric function. In this case, the transformed soil-moisture variable does not require removing trend, i.e., the roots of both denominators fell outside of the unitary circle.

2. The second step consists of performing a random search to determine the initial point for the stochastic TF. The uniform probability distribution was used to generate 1000 points over specific range, and the mean square error (MSE) was used to identify a suitable initial point, i.e., the one that exhibited a small MSE. The empirical selected range that provides satisfactory results is given by two vectors,

$$Lo = [0 \quad 0 \quad -0.9 \quad 0 \quad 0 \quad 0.1 \quad 0 \quad 12]$$

$$Up = [2 \quad 2 \quad 0.9 \quad 2 \quad 2 \quad 0.9 \quad 1 \quad 144],$$

where Lo and Up represent the minimum and maximum values, respectively, that can be assigned to the parameters, as organized in the following vector:

$$\text{parameter} = [\omega_{0,1} \quad \omega_{0,2} \quad \delta_{0,1} \quad \omega_{1,1} \quad \omega_{1,2} \quad \delta_{1,1} \quad t \quad L]$$

3. The third step consists of using the sequential quadratic programming (SQP) algorithm to estimate the parameters of the IR functions, while the L parameter is maintained fixed at a given constant value, which at the beginning is obtained by inspection (Reklaitis *et al.*, 1983; MathWorks, 2000). The SQP algorithm requires a representative sample size from a given station to derive the parameters of TF. Empirically, it was determined that 350 observations were the minimum sample size to derive reliable estimates of the TF. It should be mentioned that the sequence of 350 observations should contain several dry and wet episodes so that the algorithm will capture the soil-moisture response under the typical climate conditions.

4. This step consists of fixing the parameters of the IR function and the Hooke and Jeeves (HJ) algorithm is used to estimate the L parameter (Rekaitis *et al.*, 1983). The HJ algorithm is a function evaluation technique, i.e., a direct searching integer procedure to determine the L value that minimizes an objective function; in this case, the objective function is the MSE.

5. The last step consists of using the previous parameter values as the initial point and implementing simultaneously, the SQP and HJ algorithms to determine the complete set of parameters. This task was successfully accomplished by using the Matlab software (MathWorks, 2000).

TF Evaluation

Once the parameters of the TF models have been estimated, they are applied with rainfall radar data for a larger region. A SONN is used to identify a grid point that exhibits the similar terrain properties to a place where a soil-moisture station is located, and the identified station is called the *similar station*. The variables used to identify the similar station were: the percentage of clay, the percentage of sand, elevation, difference of surface temperature (max-min), normalized difference vegetation index (NDVI), and the accumulated rainfall of the corresponding month. The number of epoch to perform training was computed as a thousand times the number of variables and the Kohonen learning rule (Hagan *et al.*, 1996) was used to perform the train. The number of epochs was empirically derived to accomplish consistency on classification results. It should be noted that SONN uses land information to identify homogeneous land classes and the soil-moisture dynamics of each class is modeled by a TF. Thus, the SONN models land heterogeneity, but no hydrometeorology as simultaneous solution of energy mass balance at the land-atmosphere interface is computed. However, the TF uses radar data to approximate the dynamic of soil moisture near the surface and finally ANN estimates soil moisture at different depths.

Because of the fact that the TF model requires a sequence of soil moisture from a given pixel to be

initialized, a model based only on accumulated and instantaneous rainfall was developed; therefore, no soil-moisture initial conditions are required. Thus, the proposed model to create the soil-moisture initial conditions can be written as follows:

$$h_t = \rho + (\psi - \rho)(1 - e^{-g_t}), \tag{16}$$

where

$$g_t = a_0 + a_1\sqrt{R_{L_1,t}} + \left(\frac{\omega + \omega_1 B}{1 - \delta B}\right) r_t e^{-\tau_1 R_{L_1,t}} + \varepsilon_t, \quad g_t > 0 \tag{17}$$

R_{L_1},t is the cumulated rainfall at time t during the last L_1 observations. a_0 and a_1 are the trend parameters. ω, ω_1, and δ are the parameters of the IR function and τ_1 is the attenuation parameter. Equation (16) was also fitted for each station to initialize the corresponding pixels.

Once the SONN identifies the similar station, Equation (16) is used with radar rainfall data from the previous month to initialize the TF model. It was found that 540 hours of rainfall data from the previous month will capture dry and wet episodes to create a sequence of soil moisture based on rainfall. This sequence of initial values is used to create the first estimate of the h_{t-1} at time t and be able to derive the next soil-moisture values.

Soil-Moisture Profile

An effort was also devoted in this work to estimate the soil moisture at different depths, since accurate estimation of soil water dynamics at the surface and the deeper layers plays a critical role in understanding the surface and atmospheric process interactions. It should be noted that Equation (1) suggests that once the soil moisture is known at a particular layer, it can be estimated at different layers by varying the rate of change of soil moisture because of the thickness of the soil layer and taking into account of the soil and surface properties. Since the ANN has successfully been applied to model nonlinear relationships of the variables involved in a given system, it may be used to estimate the propagation of the soil-moisture rate of change at different depths.

The vertical soil-moisture profile was estimated by using an ANN that expresses the nonlinear relation between soil-moisture measurements at a specific depth (20 cm) with several measurements of soil moisture at different depths made by the SCAN. The training patterns of the neural networks are formed by the input and output vectors and can be expressed as follows:

$$P_t = \begin{bmatrix} h_{20,t} & R_m & s & c \end{bmatrix} \quad \text{and} \quad T_t = \begin{bmatrix} h_{D,t} \end{bmatrix}, \tag{18}$$

where P_t is the input vector at time t, and T_t is the output vector at time t, the output vector is also known as the target. The variable $h_{20,t}$ is the soil moisture measured at 20 cm depth at time t, and the unit of time is given in hours; the variable R_m is the accumulative rainfall in the mth month, and s, and c are the percentage of sand and clay at the given location, respectively; $h_{D,t}$ is the soil moisture at the D^{th} depth at time t.

The training patterns to study the soil-moisture variability at different depths were divided into three datasets: the first one for training, the second for testing, and the third for estimation. The training patterns included approximately 2,000 rows, the testing patterns 300 rows, and the estimation includes 700 rows. The structure of the ANN was based on searching and validation techniques that we derived in a previous work (Ramirez-Beltran and Montes, 2002). It has been shown that this procedure identifies the structure of ANN to avoid over and under training. The identified ANN structure includes four neurons in the hidden layer and one neuron in the output layer, a sigmoidal activation function in the hidden layer and a linear activation function for the output layer. The Levenberg-Marquardt algorithm was used as the learning rule and the training parameters were: 100, 0, 10^{-10} for the maximum number of epochs, the MSE, and the gradient thresholds, respectively. It was noted that most of the time, the routine terminates because it reaches the gradient threshold.

RESULTS

To apply the proposed methodology, it is necessary to study the spatial variability to classify the surface characteristics of PR and to identify which classes are associated with each of the soil-moisture stations. Once the classification is done, the corresponding "*similar station*" to each grid cell can be assigned to evaluate the associate TF model.

The SONN was used to identify the homogeneous classes and the grids that belong to the same class. In order to identify the possible number of homogeneous classes, we requested to the SONN to generate a large number of classes (i.e., to avoid ignoring some classes). In this case, we requested the creation of 20

classes; however, the SONN was only able to identify 12 homogeneous classes. We noted that in order to obtain consistent results, the number of epochs must be at least 500 var, where var is the number of training variables, and the number of epochs is the number of times that the training patterns are presented to the SONN. The training patterns were organized in a matrix, which has six columns with 8,701 rows. The columns correspond to the following training variables: clay, sand, difference in air temperature (max-min), NDVI, elevation, and cumulative monthly rainfall; and the number rows corresponded to the number of grids cells covering Puerto Rico. The number of epochs that we used was 1000 var and several replicates were conducted for testing consistency. Figure 2 shows the location of the identified 12 homogeneous classes, and Table 1 shows the average of the surface variables that characterize each class. It can be observed (Table 1) that the classes having the largest number of grid cells include classes 2, 3, and 11; whereas, the classes having the smallest number of grid cells include 6, 10, and 1.

The particular properties of each station were used to identify the class that belongs to each of them. Table 2 shows the properties and of each station. The SONN indicated that 16 stations were distributed among seven classes, and therefore; there were five classes that had no *similar station*. Fortunately, the five classes were the smallest ones and all together included only 1,635 grid cells. Table 2 shows that the Maricao and Cadena stations belong to class 2, which is the largest class in PR and has the second rank in terms of elevation (397 m), a relatively large proportion of clay (0.4), and relatively large NDVI (0.7). It should be pointed out that the numbers in parentheses of this section represent average values. Maricao and Cadena stations are similar in terms that both exhibit similar amounts of clay, and NDVI. Both stations are located within mountainous areas, but

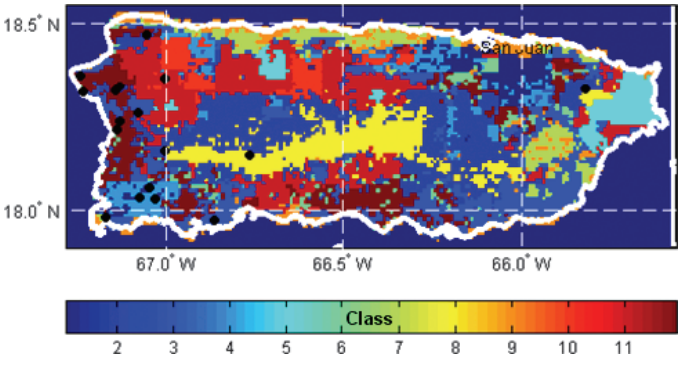

FIGURE 2. Homogenous Regions Identified in PR. Colors in the map show the location of the 12 classes.

Maricao station is located at an elevation of 746 m and Cadena station at 170 m. Although these stations showed similar averages of soil moisture, Maricao station exhibits a smaller validation error than the Cadena station. This is because of the fact that the Cadena station may have greater evapotranspiration caused by the larger daily average temperature differences (max-min), and consequently, more uncertainties on soil-moisture variability, and may be more difficult to model.

Class 9 is an interesting area that includes 754 grid cells, which ranks sixth in terms of size. Table 1 shows that this class has a large amount of sand (0.5) and the lowest NDVI (0.28), and exhibits the smallest elevation (34 m), and Table 2 shows that the following stations belong to this class: Combate, Boseque Seco, Chips, and Colegio. Table 2 shows that these stations are characterized by having the following similarities (on average): clay fraction (0.29), NDVI (0.59), and the difference in surface temperature of (8.8°C). Although the average of soil moisture was not considered as a variable to perform classification, they exhibit the smallest amount of soil moisture with an average of 22% vwc). Particularly, Combate is the station that shows the largest validation error. This is because of the fact that Combate has the largest proportion of sand (0.69), is located at a low elevation (10 m), and has a relatively small NDVI (0.57). Relatively high soil permeability, as a result of the high proportion of sand, and large temperature differences produces relatively large infiltration and significant losses as a result of strong evapotranspiration, and consequently, more soil-moisture variability. The TF model produced a significant soil-moisture underestimation. Bosque Seco station also exhibits similar properties to Combate station and shows the second largest validation error.

Class 11 is one of the most frequently encountered classes in PR and is ranked third according to size (1,269 grid cells). This class is characterized (Table 1) by the second greatest clay content (0.40), the second highest NDVI (0.72), and second highest accumulated rainfall (344 mm). There are four stations included in this class: Caobos, Edwin, Nazario, and Ramon. On an average, these stations exhibit similarities (Table 2) in the following variables: cumulative rainfall (203 mm), difference in temperature (8.9°C), and clay fraction (0.45). They also exhibit similar soil moisture with an average of 34% and similar validation error (RMSE = 2.63%).

Another of the largest classes in PR is number 3 and includes 1,386 grid cells. Table 1 shows that this class has the third highest sand content (0.31), has a relative small elevation (88 m), and a high NDVI (0.66). There are two stations in this class: Isabela and Jimenez. Table 2 shows that on an average,

TABLE 1. Soil and Surface Characteristics Over PR.

Classes	Clay	Silt	Sand	Temperature Difference (°C)	NDVI	Elevation (m)	Rainfall (mm)	Number of Grids
Class 1	0.45	0.33	0.23	14.63	0.46	59.52	214.35	345
Class 2	0.45	0.33	0.22	8.20	0.70	397.13	238.65	1526
Class 3	0.35	0.34	0.31	6.52	0.66	88.47	238.78	1386
Class 4	0.43	0.30	0.27	12.54	0.71	107.70	214.46	452
Class 5	0.41	0.36	0.23	5.91	0.64	106.09	581.76	357
Class 6	0.43	0.35	0.22	7.53	0.38	87.36	210.66	227
Class 7	0.20	0.23	0.57	7.25	0.71	91.70	292.02	416
Class 8	0.47	0.32	0.21	6.44	0.53	660.89	313.39	779
Class 9	0.25	0.24	0.50	7.62	0.28	34.63	282.12	754
Class 10	0.55	0.27	0.18	11.84	0.75	201.14	322.58	290
Class 11	0.48	0.32	0.20	7.69	0.72	177.61	344.35	1265
Class 12	0.44	0.34	0.22	6.99	0.67	61.44	190.04	904
Average	0.41	0.32	0.28	7.97	0.62	203.74	275.92	
Total number of grid cells								8701

TABLE 2. Soil and Surface Characteristics of Soil-Moisture Stations.

			Variables Used to Perform Classification					
Station Name	Class	Soil Moisture	Clay	Sand	Temperature Difference (°C)	NDVI	Elevation (m)	Rainfall (mm)
Maricao	2	0.36	0.41	0.39	6.30	0.80	746.95	150.11
Cadena	2	0.35	0.49	0.20	10.23	0.81	170.73	80.26
	Average	0.36	0.45	0.29	8.27	0.80	458.84	115.19
Isabela	3	0.28	0.47	0.43	6.48	0.73	15.24	183.64
Jimenez	3	0.28	0.23	0.55	7.32	0.79	63.72	120.90
	Average	0.28	0.35	0.49	6.90	0.76	39.48	152.27
Lajas	4	0.27	0.45	0.34	10.20	0.74	23.17	193.04
EEL	4	0.36	0.44	0.23	9.27	0.74	33.54	140.21
	Average	0.32	0.45	0.29	9.73	0.74	28.35	166.63
Combate	9	0.16	0.27	0.69	8.80	0.57	10.06	166.12
B. Seco	9	0.20	0.33	0.41	7.23	0.50	164.94	105.41
Chips	9	0.31	0.27	0.53	8.32	0.67	60.37	355.09
Colegio	9	0.21	0.31	0.61	8.61	0.61	28.05	188.98
	Average	0.22	0.29	0.56	8.24	0.59	65.85	203.90
Caobos	11	0.36	0.40	0.30	9.78	0.81	119.82	280.42
Edwin	11	0.29	0.49	0.29	8.27	0.74	133.54	289.56
Nazario	11	0.36	0.46	0.25	8.34	0.66	85.06	288.54
Ramon	11	0.33	0.47	0.35	9.33	0.67	143.90	246.89
	Average	0.34	0.45	0.30	8.93	0.72	120.58	276.35
Jamaica	12	0.24	0.47	0.25	7.85	0.69	13.72	119.89
Guilarte	8	0.41	0.51	0.19	5.73	0.66	1019.80	345.19
Yunque	2		0.43	0.19	11.30	0.76	364	229

these stations have similar soil moisture of 28% and a relatively small validation error (RMSE = 0.84).

Class 8 is ranked fifth in size, including 779 grid cells. This is the class that includes mountains (Table 1) having an average elevation of 660 m, with relatively large NDVI (0.53), small sand fraction (0.21) and a large clay fraction (0.47). Table 2 shows that Guillarte station is located on a national forest on the top of a mountain 1,019 m, with an NDVI of 0.66. The orographic characteristics and the large NDVI enhance the rainfall process, accumulating 345 mm in May 2004. Thus, the large amount of rainfall, with a large clay fraction and small temperature differences cause the soil moisture to be near to field capacity. The particular conditions of this class produce a small soil-moisture variation with fewer uncertainties, and consequently, a small validation error.

It should be noted that Jamaica station is relatively near to Jimenez station, however, the SONN classified the Jamaica station in class 12 and Jimenez station in class 3. The Jamaica and Jimenez stations are similar in the sense that they have relatively similar accumulation of rain and NDVI, as well as relatively small elevation, however, they have

different soil textures and consequently different infiltration rates. Jimenez has 0.55 and 0.23 and Jamaica has 0.25, and 0.47 sand and clay fractions, respectively. Apparently, the SONN provided more weight to texture characteristic and assigned Jamaica station to class 12.

Sixteen stochastic TF equations were derived, one for each station. Table 3 shows the parameters to initialize the model and Table 4 shows the parameter to evaluate the TF and estimate soil moisture across the island. It should be noted that El Yunque station was used to validate the model (i.e., no TF model was developed for this station). The TF model parameters depend on the surface and soil properties. Thus, the values of $\upsilon_1(B)$ and $\upsilon_2(B)$ contribute to express the memory of the soil moisture. In addition, the IR function $\upsilon_2(B)$ also contributes to transient effect of instantaneous rainfall on the soil moisture, and the τ parameter attenuates the soil-moisture response because of the cumulative rainfall during the period L.

The IR functions at Combate and Maricao stations show that both stations have a short-term memory. The first spike of $\upsilon_1(B)$ of Maricao station is negative and it is associated with $\omega_{0,1}$, and after that the IR function shows a strong exponential decay pattern with positive signs starting at lag 2 with 0.7 value and ending at about lag 11 (Figure 3a). The $\upsilon_1(B)$ at Combate station shows a large spike at lag 1 with 0.34 value and a strong exponential decay pattern starting at lag 1 and ending at lag 15. Figure 3a shows the IR function for both stations, Combate and Maricao. This figure shows that water in the soil lasts longer in Combate station because of the delta value ($\delta_{0,1} = 0.53$) being larger than the value for Maricao station ($\delta_{0,1} = 0.36$). It should be noted that $\upsilon_1(B)$ for both Maricao and Combate stations are sta-

TABLE 3. Estimated Parameters for Equation (16) to Initialize the TF Model.

Station	a_0	a_1	ω	ω_1	δ	τ_1	L_1
Maricao	0.8614	0.0252	0.0014	0.0022	0.7311	0.0739	50
Guilarte	0.9393	0.0186	0.0029	0.0004	0.1000	0.6618	12
Isabela	0.5627	0.1043	0.0077	0.0051	0.1417	0.1450	100
Combate	0.1801	0.1015	0.0433	0.0046	0.5150	0.6836	30
B. Seco	−0.2969	0.0419	0.0152	0.0035	0.5644	0.4316	32
Cadena	0.1893	0.0362	0.0084	0.0044	0.2651	0.9353	85
Caobos	0.0790	0.1051	0.0255	0.0218	0.1012	0.0564	66
Edwin	0.1525	0.0212	0.0041	0.0004	0.3098	0.8777	144
EEL	−0.0442	0.0873	0.0123	0.0117	0.1007	0.6062	77
Jamaica	0.1524	0.1107	0.0084	−0.0020	0.5116	0.7195	144
Jimenez	0.2667	0.0605	0.0114	0.0085	0.1000	0.0460	144
Lajas	−0.2363	0.1186	0.0125	0.0124	0.2481	0.7281	143
Nazario	0.5026	0.0519	0.0097	0.0082	0.1512	0.7811	102
Ramon	0.5484	0.0266	0.0085	0.0015	0.1000	0.6684	28
Chips	0.4583	0.0228	0.0057	0.0014	0.2794	0.4348	144
Colegio	−0.0570	0.0812	0.0116	0.0054	0.1328	0.9212	144

TABLE 4. Estimated Parameters of the TF Model.

Station	Dataset	$\omega_{0,1}$	$\omega_{0,2}$	$\delta_{0,1}$	$\omega_{1,1}$	$\omega_{1,2}$	$\delta_{1,1}$	τ	L
Maricao	05-2004	−0.0506	0.6869	0.36105	−0.0015	0.0108	0.1154	0.6823	34
Guilarte	05-2004	0.3821	0.8622	−0.2467	0.0023	0.0006	0.3864	0.5395	59
Isabela	05-2005	0.8301	0.3333	−0.1693	0.0031	0.0316	0.1003	0.4546	31
Combate	05-2004	0.3298	0.1000	0.5292	0.0122	0.0757	0.3000	1.0944	12
B. Seco	05-2004	1.4392	0.0491	−0.5146	0.0247	−0.0155	0.4760	0.7512	12
Cadena	05-2005	0.3601	0.1850	0.4422	0.0058	0.0106	0.1558	0.1846	14
Caobos	06-2005	0.7327	0.7950	−0.5606	0.0330	0.0283	0.1000	0.8313	47
Edwin	03-2005	0.3350	0.7845	−0.1331	0.0067	0.0031	0.1453	0.7140	28
EEL	06-2005	0.2598	0.7850	−0.0641	0.0183	0.0286	0.1011	0.5506	70
Jamaica	05-2005	1.0834	0.7978	−0.8992	0.0094	0.0211	0.1091	0.4200	12
Jimenez	04-2005	0.8028	0.4384	−0.2504	0.0122	0.0164	0.1016	0.3903	14
Lajas	06-2005	0.5550	0.8136	−0.3852	0.0175	0.0298	0.1254	1.1774	12
Nazario	05-2005	0.7989	0.7254	−0.5327	0.0100	0.0109	0.1001	1.0652	29
Ramon	06-2005	0.9866	0.6377	−0.6395	0.0223	−0.0011	0.2756	3.0833	22
Chips	04-2005	0.9116	0.4565	−0.3716	0.0046	−0.0007	0.1026	0.4047	53
Colegio	05-2005	0.8635	0.2972	−0.1761	0.0164	0.0084	0.1177	1.3842	12

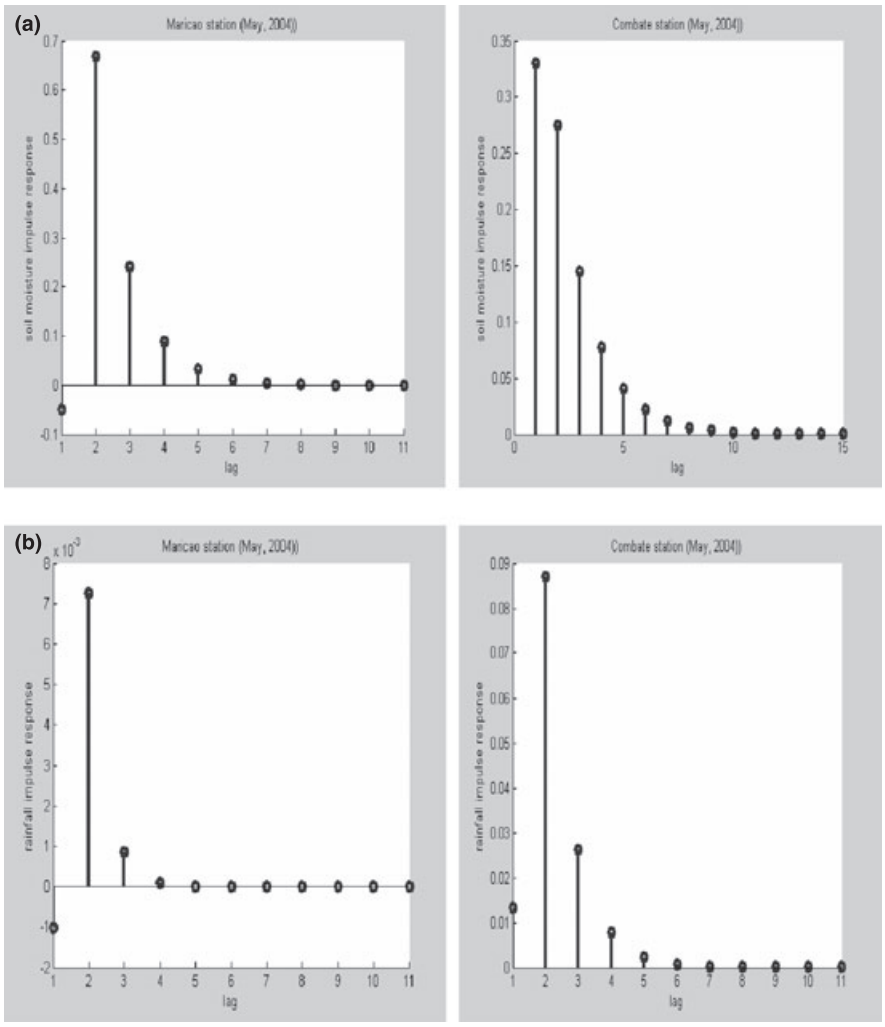

FIGURE 3. (a) The IR Function $\upsilon_1(B)$, Maricao on the Left and Combate on the Right; and (b) The IR Function $\upsilon_2(B)$, Maricao on the Left and Combate on the Right.

ble as the roots of the denominator of the response function fall outside of the unitary circle. The polynomial of the Maricao station is $1 - 0.36B = 0$, and for Combate station is $1 - 0.53B = 0$. Obviously, the roots of these polynomials fall outside of the unitary circle, and consequently, these processes are stationary. To simplify the analysis, consider the second IR function written in the following form. $\upsilon_2(B) = \frac{\omega_2(B)}{\delta_2(B)} e^{-t}$, i.e. the $R_{L,t}$ is temporarily dropped. Figure 3b exhibits the rainfall IR function for both Combate and Maricao stations and shows that $\upsilon_2(B)$ at Combate station is 10 times larger than Maricao station, indicating that instantaneous rainfall effect is 10 time stronger at the Combate station compared with Maricao station since the infiltration process is much larger in Combate than at Maricao station. It should also be pointed out that the Maricao station is close to the field capacity because rainfall occurs more frequently and this station contains a large proportion of clay. On the other hand, the L parameter for Maricao is 34 h and for Combate is 12 h. These results indicate that the $R_{L,t}$ takes the value of zero more frequently at Combate station (because of L being shorter) producing a strong soil-moisture response as a result of instantaneous rainfall effect.

Figures 4a and 4b show the observed and estimated soil moisture from the TF at Maricao and Combate stations during May 2004. Approximately, the first 360 observations of the soil-moisture station data were used to build the model to be able and capture the dry and wet episodes and the last 350 observations were used to perform model validation. As some satiations have <700 observations, the sample size for model validation was fixed at 200 to perform a fair comparison. These figures exhibit the performance of the TF model during the model fitting and validation process. Results of these stations were selected because the errors for Maricao station were

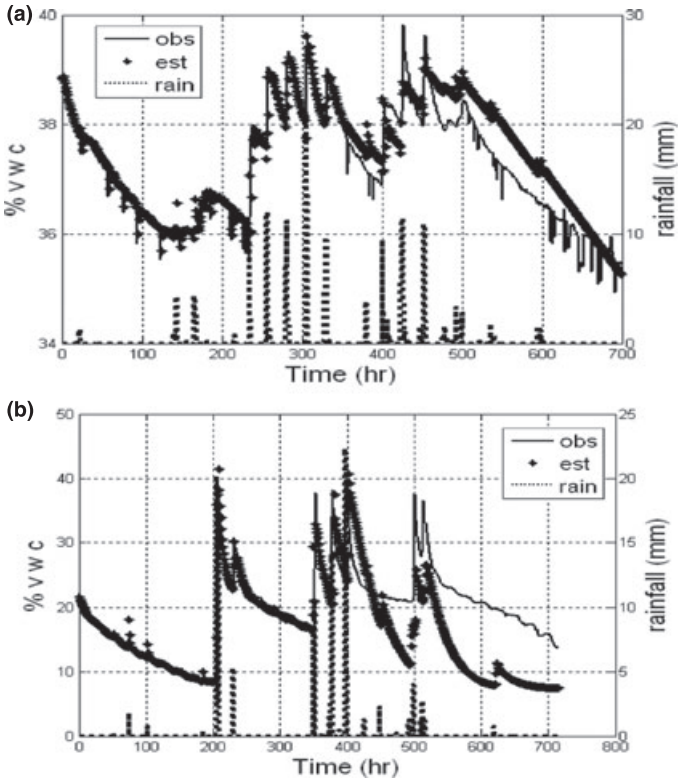

FIGURE 4. (a) Model Fitting and Validation at Maricao Station, May 2004; and (b) Model Fitting and Validation at Combate Station, May 2004. The continuous line shows the observed volumetric water content, the stars show the estimated of soil moisture, and the dotted line shows the rainfall. The first half of the series was used to develop the model and the second part of the series was used to perform validation.

smallest, and Combate station showed the highest errors (see Table 5). One possible source of error is the variance range, the larger the range the greater the uncertainty in the soil-moisture estimate. Figures 4a and 4b show that Maricao station had about 5% variation, whereas, Combate station had 35%. This range of variation occurs as a result of surface characteristics and soil properties. Maricao station is located on the top of a mountain with high rainfall, high clay content, and high NDVI, whereas, Combate station is located in the coast, with a high sand content, low rainfall and low NDVI. These latter characteristics provide the conditions for large soil-moisture response because of water infiltration and losses of soil moisture caused by evapotranspiration.

Table 5 shows model validation results in terms of the following scores of accuracy: MAE and RMSE. MAE shows the central tendency of absolute errors, whereas, RMSE shows the average variability. The average of MAE over the spatial variability was 1.96% vwc, whereas, the average of RMSE was 2.31% vwc.

To develop estimates of soil moisture, it is required to derive an initial sequential time series of soil

TABLE 5. Accuracy of Soil-Moisture Estimation at 20 cm Depth.

Station Name	RMSE (% vwc)	MAE (% vwc)
Maricao	0.53	0.47
Guilarte Forest	0.63	0.53
Isabela	0.86	0.62
Combate	8.54	7.78
Bosque Seco	3.31	3.16
Cadena	2.25	1.80
Caobos	2.61	1.54
Edwin	2.90	2.41
Exp. Estation	1.01	0.87
Jamaica	2.27	1.57
Jimenez	0.83	0.69
Lajas	2.45	2.11
Nazario	1.87	1.57
Ramon	3.14	2.74
Chips	1.82	1.69
Colegio	1.99	1.79
Average	2.31	1.96

moisture. Equation (16) with parameters shown in Table 3 was used to create the initial soil-moisture sequential values based only on hourly NEXRAD rainfall recorded during the previous month. Thus, no historical records of soil moisture for each grid cell are required to estimate soil moisture. A similar station was selected for each grid and the soil moisture for the entire island was computed by evaluating the stochastic TF Equation (9) and using parameters from Table 4. It should be noted that every grid cell should have a similar station; however, there are some grid cells that do not, and consequently, in the future, some stations will be installed within these classes. Thus, provisionally we selected a similar station based on the minimum Euclidian distance computed on the soil texture variables and elevation. In addition, there are several stations that belong to a single class and we need to decide which TF model will be assigned to a particular grid. The decision rule is based in the Euclidian distance to identify a similar station for a given pixel. A wet and a dry month were used to estimate the soil-moisture estimates across the island over two different scenarios. Figure 5a shows the PR map during 700-h average soil moisture at 1 km spatial resolution during a dry month (February 2005). Figure 5b shows the average soil-moisture estimates for PR during a wet month (May 2005). These maps show a clear distinction between a dry and a wet month. Figure 5a shows that for a dry month, most of the soil moisture ranges from 20% to 30% of vwc, whereas during a typical wet month, the soil moisture average ranges from 25% to 50% of vwc.

The closest grid to El Yunque station was identified and the surface properties were extracted and shown in Table 2. The surface characteristics indicate that El Yunque belongs to Class 2. Thus, El Yunque characteristics were compared with Cadena and

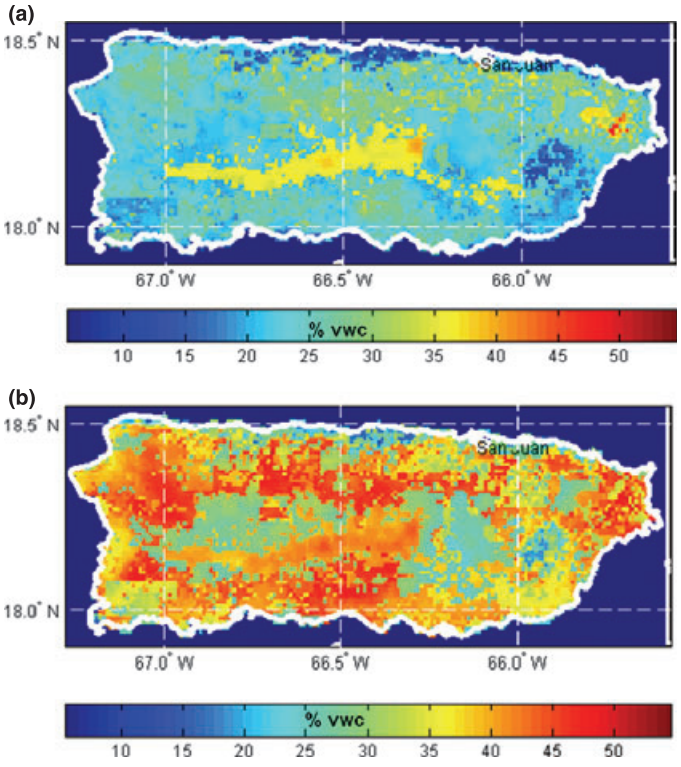

FIGURE 5. (a) Average Soil Moisture at 20 cm Depth During a Dry Month (February 2005), and (b) Average Soil Moisture for May 2005. Figures 5a and 5b show the average soil moisture during a dry and a wet month of 2005, respectively.

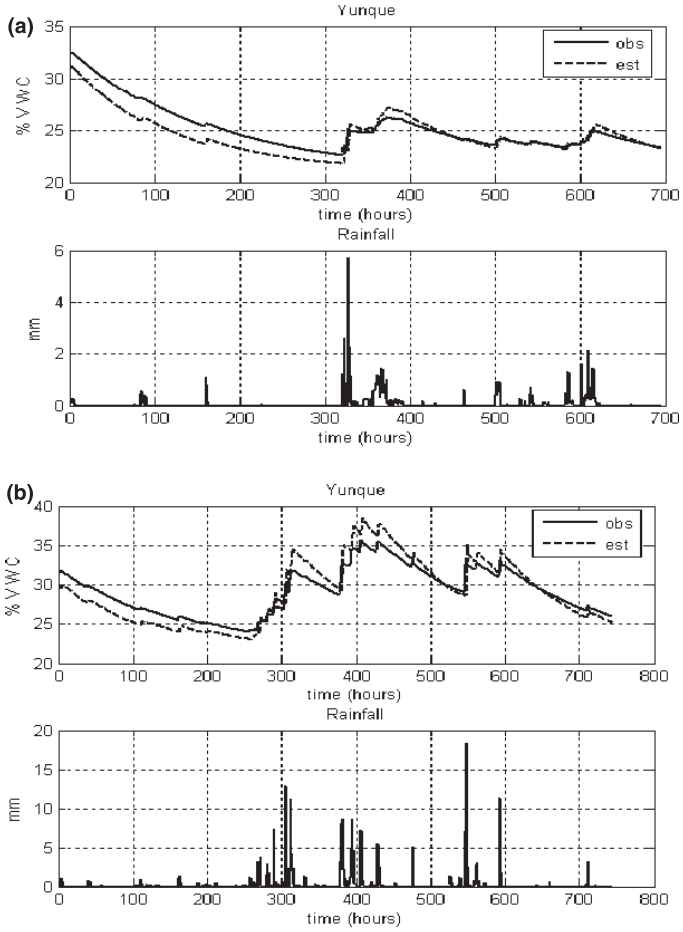

FIGURE 6. (a) Validation for El Yunque Station During February 2005; and (b) Validation for El Yunque Station During May 2005. Panel on the top of Figure 6a shows the observed and estimated soil-moisture values at El Yunque station. The panel at the bottom shows the NEXRAD hourly rainfall values. Figure 6b shows similar results as the one exhibited by Figure 6a, however, these are for a wet month. The measurements of validation statistics for the dry month were obtained as MAE = 0.82%, RMSE = 1.11%, and for the wet month were as RMSE = 1.92, MAE = 1.21.

Marico station properties and it was concluded that Cadena station exhibits the smallest Euclidian distance and it is the most *similar station* to El Yunque. Validation was conducted during a dry and a wet month for a single station. Again, the selected months were February and May 2005 for a dry and wet month, respectively. The top panel of Figure 6a shows the comparison between the observed and estimated hourly soil moisture during February 2005. The bottom panel of Figure 6a shows the observed hourly rainfall data during February 2005. Similarly, Figure 6b top panel shows comparison between observed and estimated soil moisture during a wet month and the bottom panel shows the hourly rainfall during May 2005. Although, a similar station was used to estimate soil moisture and was initialized with soil moisture generated based on rainfall, the pattern of the observed and estimated soil moisture looks very similar. The measurements of accuracy during a dry month were as follows: MAE = 0.82% and RMSE = 1.11%, and during the wet month, the measurements accuracy values were as follows: MAE = 1.20% and RMSE = 1.92% of vwc.

During the dry period, the model performed better than during the wet period. This situation may occur because the selected "similar station" reveals a small soil-moisture response under the presence of large amount of rainfall.

Once estimates were derived for a single layer, this information was used to estimate the soil moisture at different depths. The ANN was used to accomplish this task and Figure 7 shows the estimate of soil moisture at different depths for Maricao and Combate stations. Figures 7a, 7b, 7c and 7d show soil-moisture estimates at 5, 10, 50, and 100 cm depths, respectively. It should be noted that Combate and Maricao stations provide the worst and the best estimates when the TF model was applied, respectively (without the use of the ANN). On an average, the best performance of the ANN at the 5, 10, 50, and 100 cm depths was exhibited at Maricao and the worst performance was at Bosque Seco station. This result occurs

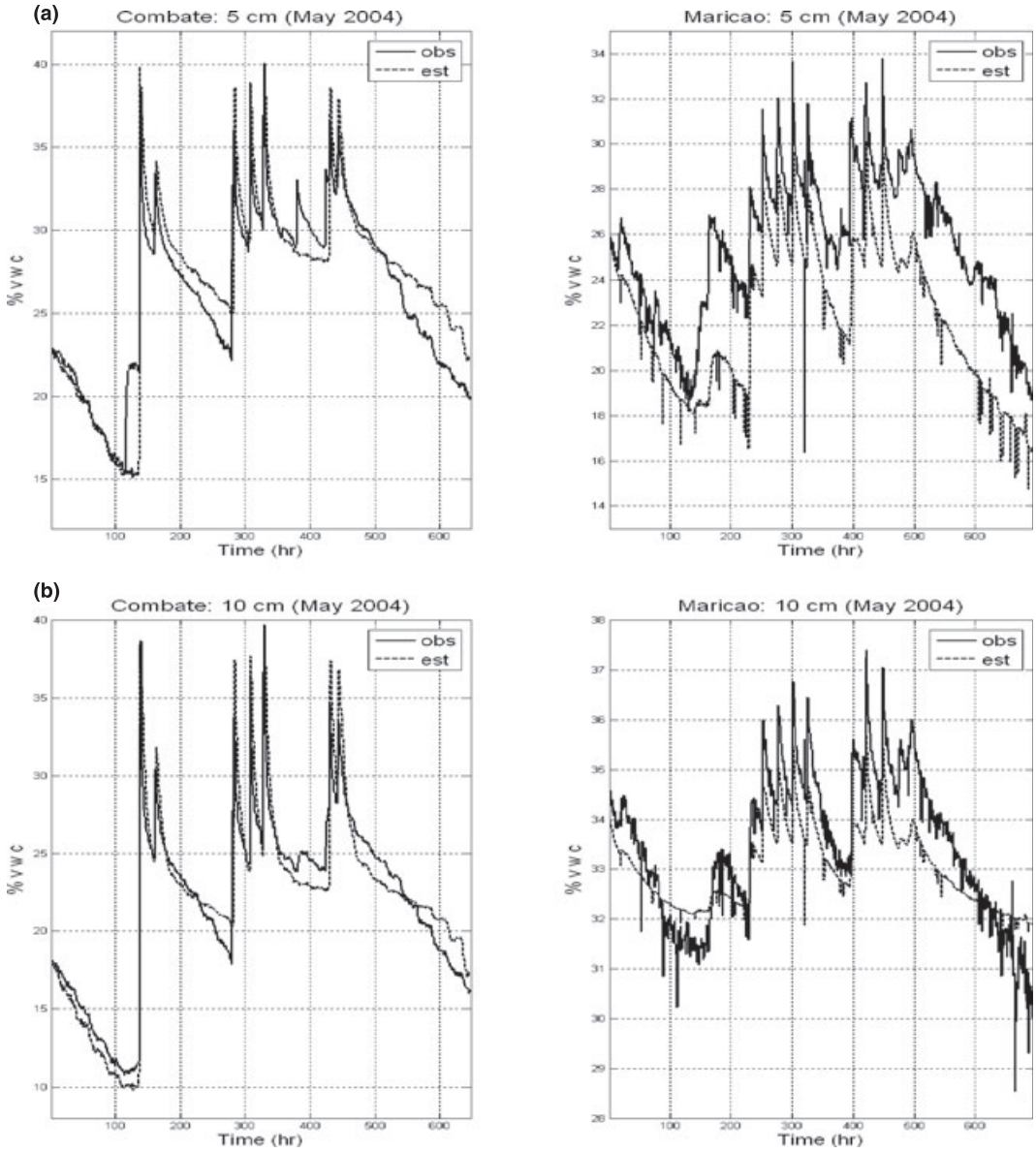

FIGURE 7. (a) Estimation of Soil Moisture at 5 cm Depth Based on 20 cm Depth, (b) Estimation of Soil Moisture at 10 cm Depth Based on 20 cm Depth, (c) Estimation of Soil Moisture at 50 cm Depth Based on 20 cm Depth, and (d) Estimation of Soil Moisture at 100 cm Depth Based on 20 cm Depth.

because of the fact that ANN has the capability of propagating the soil-moisture pattern recorded at 20 cm depth throughout soil profile. The range of variability of soil moisture at 5, 10, 50, and 100 cm depth at Maricao station were about 15, 9, 9, and 5% vwc, respectively. It should be mentioned that the soil-moisture pattern exhibited at Maricao station is similar to the observed data throughout the soil profile, only differing in magnitude. On the other hand, the range of soil-moisture variation for Combate station was: 25, 29, 17, and 0.6% vwc at 5, 10, 50, and 100 cm depth, respectively. Figure 7 shows that the soil-moisture pattern for Combate station was replicated only at the 5 and 10 cm depth, and different pattern occurred at the 50 and 100 cm depths. Therefore, the estimates of the ANN retain the soil-moisture surface pattern. Although the magnitude of the modeled values of the moisture content for the lower layer (Figures 7c and 7d) were not as good as the estimates for the surface, the results are nevertheless reasonable. For example, in the case of 100 cm depth at Combate, the maximum difference between the modeled and observed was only around 1.5% vwc. In the case of 50 cm depth for Combate, the errors are larger but were a smoothing technique to be applied (e.g., running average) the results would be sufficiently accurate for use as initial conditions in a hydrologic

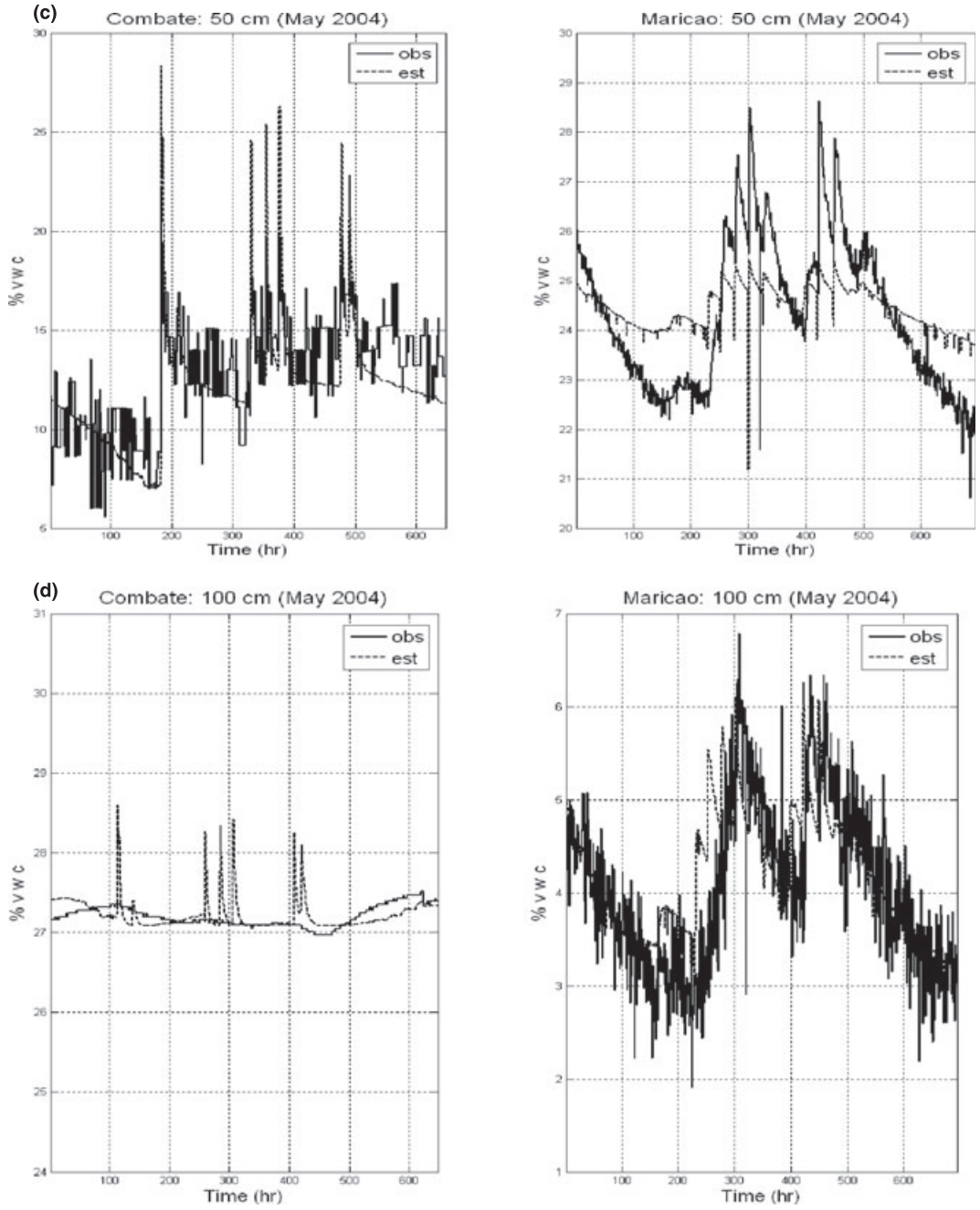

FIGURE 7. (Continued)

or atmospheric model. Table 6 shows that on an average, the RMSE for Combate station was 1.75% vwc.

As the number of stations that provide soil-moisture information for different depths is limited, the Leave-one-out cross-validation technique (Stone, 1977; Goutte, 1997) was used to measure the performance of the ANN. Table 6 shows the measurement accuracy values for each depth and for each station. Thus, the average MAE and the average RMSE as a result of depth are 2.12 and 2.50% of vwc, respectively.

POTENTIAL APPLICATIONS

The proposed soil-moisture algorithm will provide reliable soil-moisture estimates that may be used for data assimilation system, and for improving performances of atmospheric and hydrological models. Comarazamy (2001) pointed out that the performance of the regional atmospheric modeling system (RAMS) can be improved by introducing reliable soil-moisture estimates. RAMS requires soil moisture up to 1 m

TABLE 6. Accuracy of Soil-Moisture Estimates at Different Depths.

	MAE of % Volumetric Water Content				
Station Name	**5 cm Depth**	**10 cm Depth**	**50 cm Depth**	**100 cm Depth**	**Average by Station**
Bosque Seco	5.95	3.33	1.44	3.85	3.64
Combate	1.61	1.98	1.82	0.14	1.39
Guilarte	4.41	1.60	1.01	1.29	2.08
Maricao	3.26	0.77	0.97	0.51	1.38
Average by depth	3.81	1.92	1.31	1.45	2.12
Station name	RMSE of % volumetric water content				
	5 cm Depth	**10 cm Depth**	**50 cm Depth**	**100 cm Depth**	**Average by Station**
Bosque Seco	6.01	3.84	2.94	4.17	4.24
Combate	2.16	1.66	2.94	0.22	1.75
Guilarte	4.78	1.23	1.23	2.02	2.31
Maricao	3.62	0.90	1.60	0.69	1.70
Average by depth	4.14	1.91	2.18	1.78	2.50

depth to be initialized (Pielke *et al.*, 1992). The land information system (LIS) is used with numerical models to determine if short-term mesoscale numerical forecasts can be improved by using high-resolution soil moisture. Hence, our high resolution soil-moisture methodology can be applied to contribute for accomplishing the LIS/LDAS research effort.

Recently, soil moisture has been retrieved from the advanced microwave scanned radiometer (AMSR-E), which is an instrument that measures brightness temperature, which is used to generate land surface soil moisture at global scale (Njoku and Li, 1999; Njoku *et al.*, 2003). Daily products are available from the National Snow and Ice Data Center (NSIDC) since June 2002 (http://nsidc.org/data/docs/daac/ae_l2a_tbs.gd. html). However, this sensor cannot be used to estimate soil moisture over vegetated areas. Our proposed methodology may help on soil-moisture estimation as it is especially useful for estimating soil moisture over densely vegetated areas and regions characterized by having several microclimates conditions with large rainfall variability.

Although soil-moisture datasets have many applications, the observations of soil moisture are very limited. Lately, SCAN has been established to routinely collect soil moisture and to be able to study the hourly, daily, and inter annual variability of soil moisture over the U.S. Unlike soil-moisture, precipitation is measured routinely at weather stations, and also, satellite and radar are utilized for measuring rainfall over large areas at long period and at high sampling frequency. Thus, the proposed methodology can be used in conjunction with satellite rainfall to estimate soil moisture at high resolution over large areas. For instance, the Hydro-Estimator (HE) which is a high resolution rainfall retrieval algorithm that uses information from Geostationary Operational Environmental Satellite (GOES) and from numerical whether prediction models to produce rainfall rates (Vicente *et al.*, 1998; Scofield and Kuligowski, 2003). The HE uses brightness temperatures data from the infrared window channel (10.7 μm) to estimate rainfall rates every 15 min at 4 km spatial resolution over U.S. and its territories, including PR. It should be pointed out that the HE provides rain rates with similar spatial and temporal resolution as the NEXRAD. Therefore, our proposed methodology will be a straightforward application to derive soil-moisture estimates from satellite rainfall data.

SUMMARY AND CONCLUSIONS

This paper presents a new and practical alternative to estimate soil moisture. The model is based mainly on a stochastic representation of the Richard's equation and on the observation that rainfall is the fundamental variable to estimate soil-moisture variability, and this observation has been confirmed with sampling field measurements. The model includes soil texture, elevation, difference of surface temperature (max-min), and rainfall observations, and has the capability of incorporating other variables such as hourly temperature, and wind components. Model validation over spatial variability shows an average RMSE of 2.31% vwc.

The proposed stochastic TF model estimates the spatial and temporal variability of soil moisture. The TF model for a particular grid is selected by using a SONN, which identifies similarities of the surface spatial variability. Once similarities of spatial variability are found the TF model is initialized with soil-moisture information derived from cumulative rainfall obtained by NEXRAD. The SONN identifies

similarities by using the following discriminate variables: accumulative precipitation of the current month, soil texture, surface temperature, vegetation index, and elevation.

The first 350 observations (approximately) of a given station were used to develop the TF model and the remaining 350 observations were used to validate the model. The TF models were developed by using 16 stations that are located in the western part of PR. Data from one station not included in the model building process was used to conduct the second validation exercise. This station is located in the eastern part of PR over the National Rainforest (El Yunque). The TF model was used to estimate the soil moisture during 700 hours during dry and wet conditions at this location and results were compared with observed soil moisture from the station. The validation accuracy was measured by the RMSE with a value of 1.11% vwc during a dry month and 1.92% vwc during a wet month.

The proposed methodology not only estimates the spatial and temporal variability of soil moisture but also provides soil moisture at vertical depths up to 1 m depth. A feedforward ANN was used to estimate soil moisture at four different depths (5, 10, 50, and 100 cm). The ANN uses the known soil moisture at 20 cm depth, the soil texture, and accumulative rainfall to estimate the soil-moisture profile. The leave-one-out validation technique was used to measure the accuracy of the ANN, and the RMSE over the vertical profile were 2.5% of volumetric water content. Validation results showed that the proposed algorithm is a potential tool to estimate hourly soil moisture at 1 km resolution with up to 1 m depth.

ACKNOWLEDGMENTS

This research has been supported by the NOAA-CREST grant NA17AE1625, by the NASA-EPSCoR grant NCC5-595, by the NSF grant No. 0313747, by the NOAA-NWS grant NA06NWS4680011, and also by the University of Puerto Rico at Mayaguez. Authors appreciate and recognize the funding support from these institutions. We want to recognize the important recommendations from the anonymous reviewers to improve the manuscript. We also want to express our sincere recognition to Pieter van der Meer for his invaluable contribution to improve the manuscript.

LITERATURE CITED

Balsamo, G., F. Bouyssel, and J. Noilhan, 2004. A Simplified Bi-Dimensional Varaitional Analysis of Soil Moisture From Screen-Level Observations in a Mesoscale Numerical Weather Prediction Model. Quarterly Journal of Royal Meteorological Society 130:895-915.

Belair, S., G. Balsamo, J-F. Mahfouf, and G. Deblonde, 2005. Toward the Inclusion of Hydros Soil Moisture Measurements in Forecasting Systems of the Meteorological Service of Canada. *In:* Geoscience and Remote Sensing Symposium, 2005, IGARSS 2005, Proceedings of the 2005 IEEE International, pp. 2741-2743.

Box, G.E.P. and G.M. Jenkins, 1976. Time Series Analysis Forecasting and Control. Holden-Day, Oakland, California.

Breidenbach, J.P. and J.S. Bradberry, 2001. Multisensor Precipitation Estimates Produced by the National Weather Service River Forecast Centers for Hydrologic Applications. Proceedings 2001 Georgia Water Research Conference, Institute of Ecology, University of Georgia, Athens, Georgia.

Brockwell, P.J. and R.A. Davis, 2002. Introduction to Time Series and Forecasting (Second Edition). Springer-Verlag, New York, New York.

Castelli, F., I. Rodriguez-Iturbe, and D. Entekhabi, 1996. An Analytical Framework for the Modeling of the Spatial Interaction Between the Soil Moisture and the Atmosphere. Journal of Hydrology 184:19-34.

Cemek, B., R. Meral, M. Apan, and H. Merdum, 2004. Pedotransfer Function for the Estimation of the Field Capacity and Permanent Wilting Point. Pakistan Journal of Biological Sciences 7(4):535-541.

Comarazamy, D.E., 2001. Atmospheric Modeling of the Caribbean Region: Precipitation and Wind Analysis in Puerto Rico for April 1998, Master Thesis, Department of Mechanical Engineering, University of Puerto Rico, Mayaguez, Puerto Rico.

DHI Software, Inc., 2003. Mike She User Guide. Agern Allé 5, DK-2970 Hørsholm, Denmark, dhi@dhigroup.com. 174 pages.

Dinar, A., K.C. Knapp, and D.J. Rhoades, 1986. Production Function for Cotton With Dated Irrigation Quantities and Qualities. Water Resources Research 22:1519-1525.

Downer, C.W., E.J. Nelson, and A. Byrd, 2003. Primer: Using Wathershed Modeling System (WMS) for Gridded Surface Subsurface Hydrologi Analysis (GSSHA) Data Development - WMS 6.1 and GSSHA 1.43C. ERDC/CHL TR-03-02. U.S. Army Corps of Engineers, Coastal and Hydraulics Laboratory.

Entekhabi, D. and I. Rodriguez-Iturbe, 1994. Analytical Framework for the Characterization of the Space-Time Variability of Soil Moisture. Advances in Water Resources, 17(1-2):35-45.

Ewel, J.J. and L. Whitmore, 1973. The Ecological Life Zones of Puerto Rico and the U.S. Virgin Islands. U.S. Department of Agriculture Forest Service Research Paper ITF-18. Institute of Tropical Forestry, Rio Piedras, Puerto Rico.

Fan, Y., H.M. van den Dool, K. Mithchell, and D. Lohmann, 2002. NWS-CPC's Monitoring and Prediction of U.S. Soil Moisture and Associated Land Surface Variables: Land Data Reanalysis. Proceedings of the 27th Annual Climate Diagnostics and Prediction Workshop. October 21-25, 2002, George Mason University, Fairfax, Virginia.

Fulton, R.A., J.P. Breidenbach, D.J. Seo, and D.A. Miller, 1998. The WSR-88D Rainfall Algorithm. Weather Forecasting, 13:377-395.

Goutte, C., 1997. Note on Free Lunches and Cross-Validation. Neural Computation, 9:1211-1215.

Gill, M.K., T. Asefa, M.W. Kemblouski, and M. McKee, 2006. Soil Moisture Prediction Using Support Vector Machines. Journal of American Water Resources Association 42(4):1033-1046.

Hagan, M.T., H.B. Demuth, and M. Beal, 1996. Neural Network Design. PWS Publishing Company, Boston, Massachusetts.

Hamilton, J.D., 1994. Time Series Analysis. Princeton University Press, Princeton, New Jersey.

Helmer, E.H., 2002. Mapping the Forest Type and Land Cover of Puerto Rico, a Component of the Caribbean Biodiversity Hotspot. Caribbean Journal of Science 38(3-4):165-183.

Huang, J., H. van den Dol, and K.P. Georgakakos, 1996. Analysis of Model-Calculated Soil Moisture Over the United States

(1931-93) and Application to Long-Range Temperature Forecasts. Journal of Climate 9(6):1350-1362.

Hunter, S.M., 1996. WSR-88D Radar Rainfall Estimation: Capabilities, Limitations and Potential Improvements. National Weather Digest 20:26-38.

Jiang, H. and W.R. Cotton, 2004. Soil Moisture Estimation Using an Artificial Neural Network: A Feasible Study. Canadian Journal of Remote Sensing 30(5):827-839.

Klazura, G.E., J.M. Thomale, D.S. Kelly, and P. Jendrowski, 1999. A Comparison of WsR-88D Rain Estimates UIT Gauge Measurements for High and Low Reflectivity Gradient Precipitation Events. National Weather Service, Honolulu, Hawaii.

Kumar, P., 2004. Layer Average Richard's Equation With Lateral Flow. Advances in Water Resources 27:521-531.

Lee, D.H. and L.M. Abriola, 1999. Use of the Richards Equation in Land Surface Parameterization. Journal of Geophysical Research 104(D22):27519-27526.

Margulis, S.A., D. McLaughim, D. Entekhabi, and S. Dunne, 2002. Land Data Assimilation and Estimation of Soil Moisture Using Measurements From the Southern Great Plains 1997 Field Experiment. Water Resources Research 38(12):1299.

MathWorks, 2000. Optimization Toolbox for Use With Matlab: User's Guide. The MathWorks, Inc., Natick, Massachusetts.

McKee, S.R., J.D. Kalma, S.W. Franks, and Y. Shao, 2001. The Relationship Between Temporal Surface Temperature Trends and Soil Moisture Status: An Exploratory Study With a Coupled Landsurface-Atmosphere Model. IEEE 2001:1312-1314.

Mehrotra, R., 1999. Sensitivity of Runoff, Soil Moisture and Reservoir Design to Climate Change in Central Indiana River Basins. Climate Change 42:725-757.

Njoku, E.G., T.J. Jackson, V. Lakshmi, T.K. Chan, and S.V. Nghiem, 2003. Soil Moisture Retrieval From AMSR-E. IEEE Transactions on Geoscience and Remote Sensing 41(2):215-229.

Njoku, E.G. and L. Li, 1999. Retrieval of Land Surface Parameters Using Passive Microwave Measurements at 6-18 GHz. IEEE Transactions on Geoscience and Remote Sensing 37(1):79-93.

Pan, F., C.D. Peters-Lidard, and M.J. Sale, 2003. An Analytical Method for Predicting Surface Soil Moisture From Rainfall Observations. Water Resources Research 39(11):1314, doi:10.1029/2003WR002142, 2003.

Pandit, S.M. and S.M. Wu, 1983. Time Series and Systems Analysis With Applications. John Wiley and Sons, New York.

Pielke, Sr., R.A., W.R. Cotton, R.L. Walko, C.J. Tremback, W.A. Lyons, L.D. Grasso, M.E. Nicholls, M.D. Wesley, T.J. Lee, and J.H. Copeland 1992. A Comprehensive Meteorological Modeling System- RAMS. Meteorology and Atmospheric Physics 49: 69-91.

Ramirez-Beltran, N.D. and J.A. Montes, 2002. Neural Networks to Model Dynamic Systems With Time Delays. IIE Transactions 34:313-327.

Reklaitis, G.V., A. Ravindran, and K.M. Ragsdell, 1983. Engineering Optimization: Methods and Applications. John Wiley and Sons, New York, New York.

Robock, A., L. Luo, E.F. Wood, F. Wend, and K.E. Michael 2003. Evaluation of the North American Land Data Assimilation System Over the Southern Great Plain s During the Warm Season. Journal of Geophysics Research 28, (D22):8846. doi: 10.1029/2002ID003309.

Ross, M., J. Geurink, P. Tara, K. Trout, and T. Jobes, 2004. Integrated Hydrologic Model (IHM) Volume 1: Theory Manual, Prepared for Tampa Bay Water Publication Number USF-CMHAS 0383.0304.58, University of South Florida, Tampa, Florida.

Satalino, G., F. Mattia, M.W.J. Davidson, T.L. Toan, G. Pasquatiello, and M. Borgeaud, 2002. On Current Limits of Soil Moisture Retrieval From ERS-SAR Data. IEEE Transactions on Geosciences and Remote Sensing 40(11):2438-2447.

Scofield, R.A. and R.J. Kuligowski, 2003. Status and Outlook of Operational Satellite Precipitation Algorithms for Extreme-Precipitation Events. Weather and Forecasting 18:1037-1051.

Spiegel, M.R., 1994. Calculus of Finite Differences and Difference Equations, Schaum's Outline Series. McGraw-Hill, Inc., New York, New York.

Stone, M., 1977. Asymptotics for and Against Cross-Validation. Biometrika 64:29-35.

Strait, S., K.E. Saxton, and R.I. Papendick, 1979. Pressure and Hydraulic Conductivity Curves for Various Soil Textures. Internal Report. USDA-ARS, Washington State University, Pullman, Washington.

Van den Dool, H., J. Huang, and Y. Fan, 2003. Performance and Analyses of the Constructed Analogue Method Applied to U.S. Soil Moisture Over 1981-2001. Journal of Geophysical Research, 108:1-16.

Vicente, G.A., R. Scofield, and W.P. Menzel, 1998. The Operational GOES Infrared Rainfall Estimation Technique. Bulletins of the American Meteorological Society 79:1883-1898.

Viterbo, P. and A.K. Betts, 1999. Impact of the ECMWF Reanalysis Soil Water on Forecasts of the July 1993 Mississippi Flood. Journal of Geophysics Research 104(D16):19,361-19366.

Walker, J.P. and P.R. Houser, 2004. Requeriments of a Global Near-Surface Soil Moisture Satellite Mission: Accuracy, Repeat Time, and Spatial Resolution. Advances in Water Resources 27:785-801.

Walker, J.P., G.R. Willgoose, and J.D. Kalma, 2002. Three-Dimensional Soil Moisture Profile Retrieval by Assimilation of Near-Surface Measurements: Simplified Kalman Filter Covariance Forecasting and Field Application. Water Resource Research, 38(12):1301.

Wei, W.S., 1990. Time Series Analysis: Univariate and Multivariate Methods. Addison-Wesley, Redwood City, California.

Westrick, K.J., C.F. Mass, and B.A. Colle, 1999. The Limitations of the WSR-88D Radar Network for Quantitative Precipitation Measurement Over the Western United States. Bulletins of the American Meteorological Society 80:2289-2298.

Yeh, G.T., H.P. Cheng, J.R. Cheng, H.C.J. Lin, and W.D. Martin, 1998. A Numerical Model Simulating Water Flow and Contaminant and Sediment Transport in WAterSHed Systems of 1-D Stream-River Network, 2-D Overland Regime, and 3-D Subsurface Media (WASH123D: Version 1.0), Technical Report CHL-98-19, U.S. Army Corps of Engineering, Waterway Experiment Station, Vicksburg, Mississippi.

Zongqian, L., T. Yuhua, and L. Ning, 2000. Inversion of the Soil Moisture Based Upon Neural Network. *In:* IEEE, Antennas, Propagation and EM theory, 2000. Proceedings of the ISAPE 2000, 5th International Symposium, Beijing, China, pp. 398-400.